



Research article

UDC 624.131.436

DOI: 10.34910/MCE.114.3



Model of soil thermal conductivity in the form of a truncated sphere

A.V. Zakharov¹ , A.B. Ponomaryov¹ , I.V. Ofrikhter² 

¹ Saint-Petersburg Mining University, St. Petersburg, Russia

² Perm National Research Polytechnic University, Perm, Russia

✉ av_zaharov@mail.ru

Keywords: theoretical analysis, theoretical prediction model, thermal conductivity, porosity, soil, thermal conductivity model

Abstract. The model is designed for a three-phase soil system: mineral part, water, and air. The model's input parameters are porosity and water saturation coefficient, which characterize the volumetric ratio of the main components in the soil. The soil thermal conductivity model is represented as a sphere of the mineral part in the sphere of water. A cube - a unit volume, truncates both spheres. The main design parameters are the radii of the spheres of water and air. A single volume was divided into several heat flow paths with the same set of soil components, for each of which the thermal conductivity was calculated as for a multilayer wall. The total thermal conductivity was calculated by averaging, taking into account the cross-sectional areas of each of the paths. Depending on the values of the design parameters and their relationship, the model has identified three design cases. An analytical solution is obtained for each design case. Comparison of the calculation results using the developed model showed good agreement with experimental data and existing thermal conductivity models.

Funding: This research was carried out with the financial support of the Ministry of Science and Higher Education of the Russian Federation in the framework of the program of activities of the Perm Scientific and Educational Center "Rational Subsoil Use".

Citation: Zakharov, A.V., Ponomaryov, A.B., Ofrikhter, I.V. Model of soil thermal conductivity in the form of a truncated sphere. Magazine of Civil Engineering. 2022. 114(6). Article No. 11403. DOI: 10.34910/MCE.114.3

1. Introduction

Thermophysical properties play an essential role when performing calculations of energy-efficient structures of foundations of foundation soils [1]. The main thermophysical properties of the soil are usually referred to as thermal conductivity λ and heat capacity c .

The thermophysical properties of soils depend on many factors: the mineral of the soil particles, the size and shape of the particles, density, moisture content, porosity.

Solid minerals are the most heat-conducting components in the air-water-soil particles system. Therefore, they define an upper limit for thermal conductivity. The soil, consisting of different mineral substances, has different thermal conductivity [2]. Soil with a higher quartz content has a higher thermal conductivity [3].

The heat flux between soil particles is proportional to the radius of the particles. Larger particles and smaller contacts in a given volume allow one to obtain a higher thermal conductivity [2], [4]. An increase in thermal conductivity is provided by smaller particles filling the pore space between large ones [5].

An increase in soil density (constant particle size distribution) leads to a decrease in porosity, an increase in soil particles' contact area, and an increase in its thermal conductivity. The moisture content of the soil significantly affects its thermal conductivity. With increasing humidity, the thermal conductivity of the soil increases.

There are two main approaches to determining the thermal conductivity of soils. Conditionally they can be called direct and calculated.

With a direct approach, the measurement of the thermal conductivity of a particular soil sample is carried out in laboratory conditions. As a result, the thermal conductivity of the soil is determined at specific values of the physical characteristics (density, the density of dry soil, moisture, etc.).

The computational approach includes a large group of methods based on determining the thermal conductivity of the soil by calculating it from the previously established dependence of the thermal conductivity of the soil on its physical characteristics, the thermal conductivity of its components, taking into account their volume fraction.

Much research has been devoted to determining the dependence of the thermal conductivity of soil on its physical characteristics. Based on the results of which, a variety of computational models and methods have been proposed. At the same time, it is noted that new models are currently appearing, which indicates that a universal model has not been found.

The existing methods and models can be divided into three groups [6]:

- Mixing models. These models view the soil as a multiphase system composed of water, air, and soil particles. The thermal conductivity of the soil is calculated as a combination of the thermal conductivity of the volumes of individual phases (components) in an elementary volume;
- Empirical models. These models are based on the identification of empirical dependences of the thermal conductivity of the soil on its physical characteristics (density, moisture, porosity, etc.);
- Mathematical models. These models were borrowed from predictive models for other physical properties such as dielectric constant, magnetic permeability, electrical conductivity, and hydraulic conductivity.

In mixing models, the soil is most often considered a medium consisting of three main components: water, air, soil particles. Ice is added in the models for soils in a frozen state instead of or together with water.

Some of the models allow to include an unlimited number of components (for example, take into account organic inclusions). In contrast, others, on the contrary, are developed for a specific set and number of components.

The most common models are based on the classical laws of mixing (arithmetic and geometric): sequential, parallel, geometric mean model, quadratically parallel, effective mean, etc.

The simplest models are sequential ones. These models have the least amount of constraints as they do not consider the actual soil structure. The sequential model provides constant heat flux through each series-connected component so that each component has a different temperature gradient determined by its thermal conductivity.

Mixing models include Mickley (1951) [7], De Vries (1952) [8], Gemant (1952) [2], McGaw (1969) [9], many of which were later upgraded or formed the basis of new models.

Mixing models also include Gori and Corasaniti (2002) [10], Campbell (1994) [11], Gens et al. (2009) [12], Cho et al. (2001) [13], Haigh (2012) [14], Tarnawski and Leong (2016) [15], Tian et al. (2016) [16], Lu et al. (2014) [17].

One of the first empirical models for assessing thermal conductivity was the Kersten model [18]. Another of the well-known empirical methods for determining the thermal conductivity of soils is the method of Johansen (1975) [19]. This model is developed by Knutsson (1983) [20], Coté and Konrad (2005) [21], Nikoosokhan et al. [22], Zhang et al. (2017) [23], Lu et al. (2014) [17], Dharssi et al. (2009) [24], Wilson et al. (2011) [25], Róžański and Stefaniuk (2016, 2020) [26], [27].

The empirical models also include the models of McCumber and Pielke (1981) [28], Kahr and Muller-Vonmoos (1982) [29], Campbell (1985) [11], Chung and Horton (1987) [30], Becker (1992) [31], Newson et al. (2002) [32], Chen (2008) [14], Caridad et al. (2014) [33], Lu et al. (2014) [17], Yoon et al. (2018) [34].

Among the mathematical models are the models, Nimick and Leith (1992) [35], Jougnot and Revil (2010) [36].

In order to compare the various calculation methods, several assessments of the thermal conductivity of the soil have been performed. A calculation was made for sandy and clayey soil with a dry soil density $\rho_d = 1.4 \text{ g/sm}^3$, soil particle density $\rho_s = 2.65 \text{ g/sm}^3$ and varying the saturation S_r in the range $0.01 \div 1.00$. More than 60 methods were used for the calculation. The calculation results are presented on Figures 1 and 2.

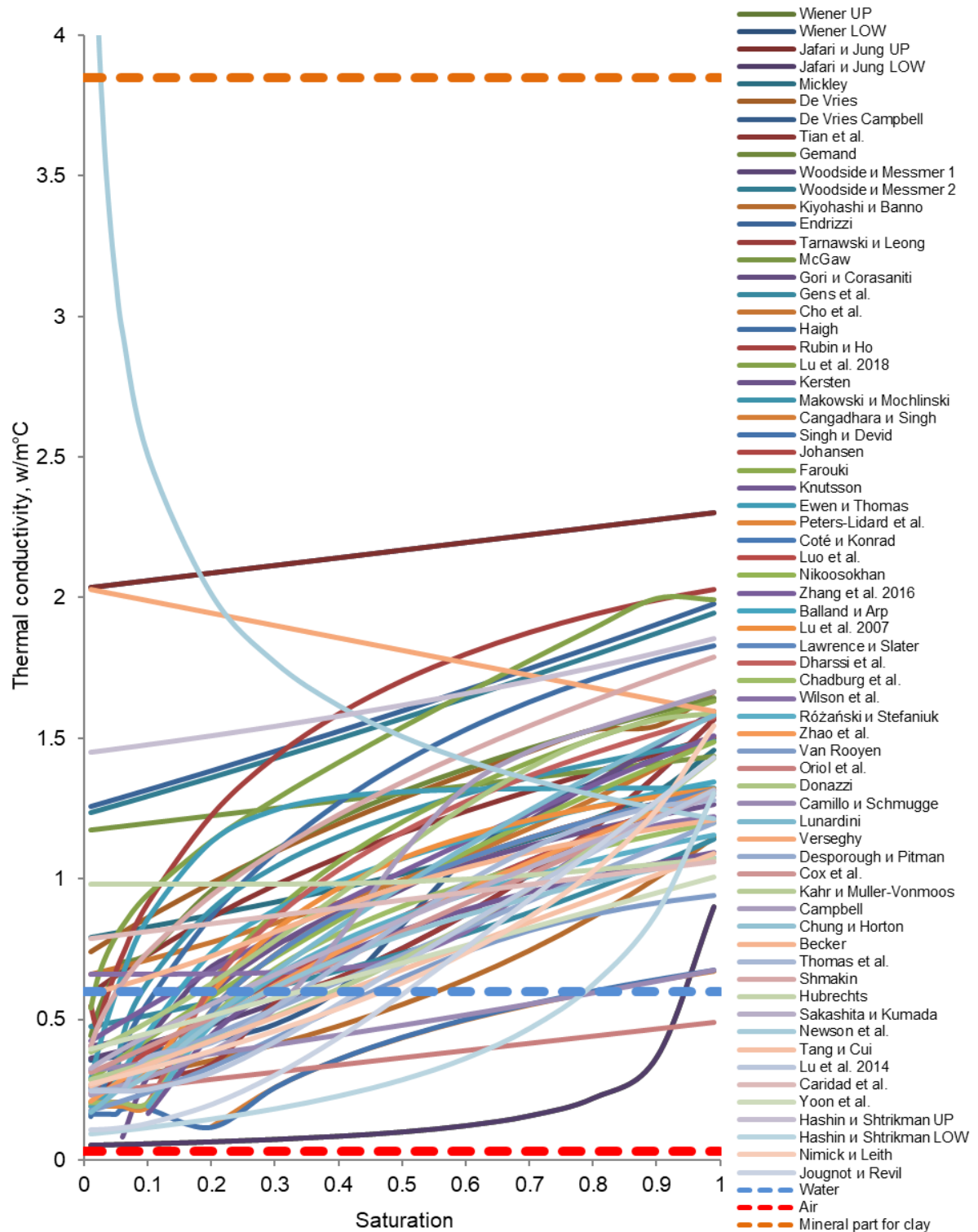


Figure 1. Thermal conductivity of clay soil ($\rho_d = 1.4 \text{ g/sm}^3$, $\rho_s = 2.65 \text{ g/sm}^3$) with a saturation from 0.01 to 1, calculated according to various models.

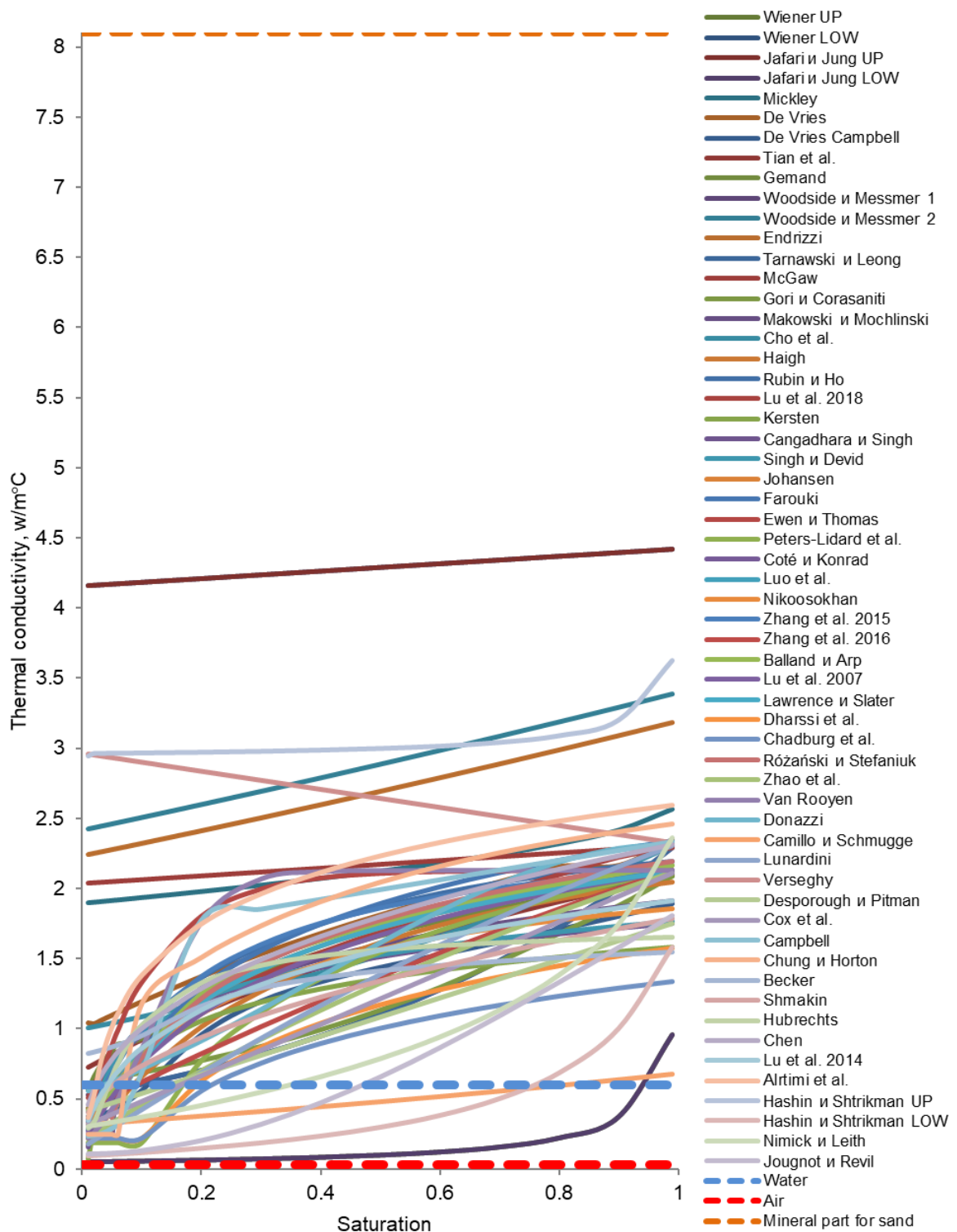


Figure 2. Thermal conductivity of sand soils ($\rho_d = 1.4 \text{ g / sm}^3$, $\rho_s = 2.65 \text{ g / sm}^3$) with a saturation from 0.01 to 1, calculated according to various models.

The analysis of the graphs showed that the considered models give a wide range of soil thermal conductivity values with the same input parameters. In this case, the obtained values lie within the Wiener boundaries (for the overwhelming number of models). A wide range of values may be due to:

- Some empirical models were developed for soils of a certain granulometric and, probably, more importantly, mineralogical composition. Since the thermal conductivity of particle minerals can differ significantly (from 2 W/m°C to 9 W/m°C). In addition, the features of the origin and composition, the presence of organic impurities (and others) in the soils, based on the tests of which empirical dependencies and empirical correction factors were obtained;

- Empirical models were developed or verified on an array of experimental studies of soils with a specific range of their physical characteristics (dry soil density, moisture content or saturation, etc.);
- Assumptions and simplifications can cause more significant errors than they supposed.

After analyzing the above studies, it can be concluded that at the moment, there is no generally accepted method for calculating the thermophysical characteristics of the soil. Existing methods give a wide range of estimates.

Empirical techniques based on experimental data give more accurate results for a specific type of soil (with certain limits of variation of its physical characteristics, grain size and mineralogical composition, etc.). Computational models (mathematical and displacement models), which attempt to describe the process mathematically conductivity in soils, give less accurate results, but have a wider field of application.

Thus, the research goal was set: the development of a non-empiric method for calculating the thermal conductivity of soil based on its physical characteristics. The following problems were solved:

- a model of soil heat transfer is proposed;
- analytical solutions of the parameters of the developed model were obtained, and a calculation method was proposed;
- laboratory studies were carried out to determine the thermal conductivity of sandy and clayey soils;
- the analysis of the convergence of the data obtained by the developed method with experimental data has been carried out.

2. Methods.

The mechanism of heat transfer between its particles is essential in describing the heat transfer process in soils. Existing researches register that heat transfer between particles occurs in several directions (Figure 3) [37].

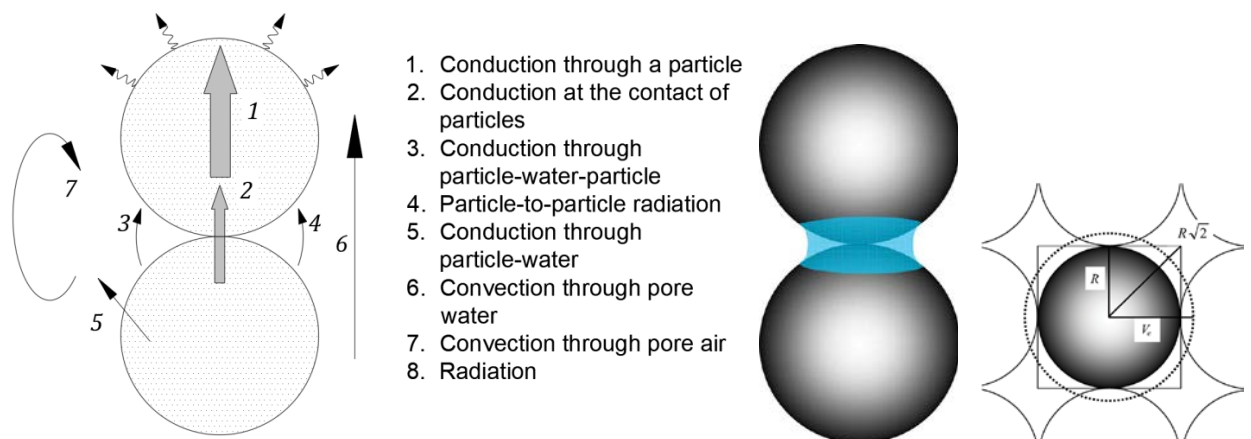


Figure 3. Scheme of heat transfer between soil particles and spherical model of soil particles [38].

At the same time, the experimental data have inconsistencies with the model of soil particles in the form of spheres. This is explained by the fact that the leading share of heat transfer is due to conductive heat transfer between particles, and the contact area of original soil particles is much higher, including due to bound water at the contact site (Figure 3).

Numerical heat transfer modeling at the contact of spherical particles considering a water lens shows a high convergence with experimental data, but only for soils with low moisture content [38]. The thermal conductivity of the soil at higher humidity is influenced by gravitational water, the position of which is not described by this model.

The proposed soil model is a sphere, truncated by the sides of a unit cube (Figure 4) to consider the increase in the contact areas of a part of the soil, the characteristics of the mineral part, and the presence of water. This model is not entirely new. Many researchers have used a spherical soil model to estimate thermal conductivity [38], [39]. Previously, the authors determined a method for refining a number of characteristics of spherical model based on laboratory tests [40]. However, in this study, it is proposed to expand the scope of the model, in comparison with existing analogues. For the proposed model, the following assumptions are made:

- Only conductive heat transfer is considered because of the possibility of experimental testing of such a model in laboratory conditions. This assumption is often used to determine the effective thermal conductivity of multiphase materials.
- It is assumed that the soils have an above-zero temperature without significant temperature gradients. Thus, heat exchange associated with a change in the state of aggregation of the liquid phase, water movement, or steam movement is ignored.
- A truncated sphere that imitates the mineral part of the soil is not related to the size of the soil particles but only expresses the volume fraction of the mineral part.
- Soil particles have contact areas with each other.

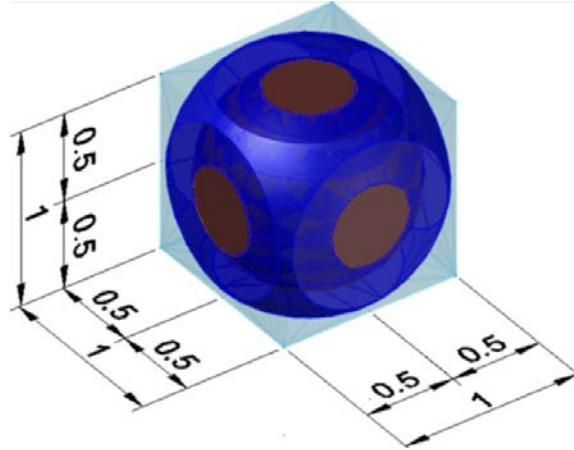


Figure 4. Geometric model of a soil particle in a unit volume.

The soil model has three main components: mineral, water, and air. The volume of each component is calculated from the porosity n and the saturation S_r , which are the model's input parameters.

$$\begin{aligned} V_s &= 1 - n; \\ V_w &= n \cdot S_r; \\ V_a &= n \cdot (1 - S_r) \end{aligned} \quad (1)$$

where V_s is the mineral volume, V_w is the water volume, V_a is the pore volume. The calculated parameters of the model are taken as R_s and R_w are radiuses of the spheres forming the volumes of the mineral part and water, respectively.

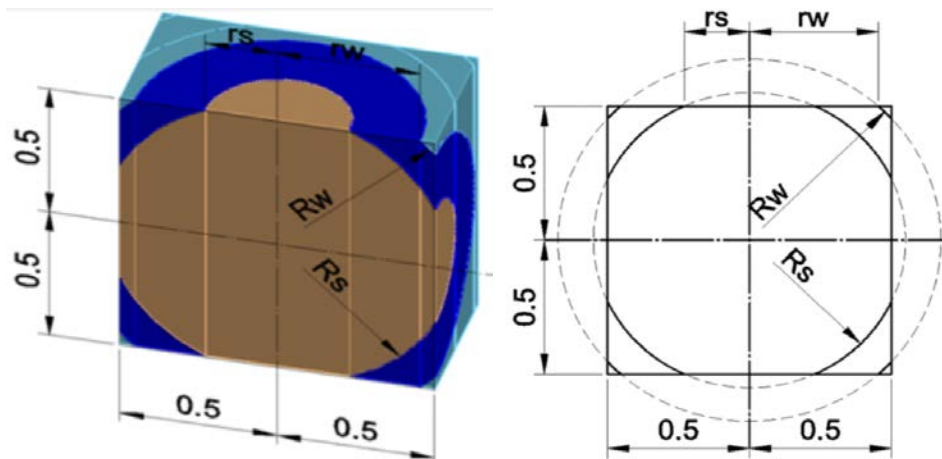


Figure 5. The design scheme of the model.

R_s is the radius of the mineral part sphere. R_w is the radius of the sphere that forms the volume of groundwater. The radius r_s of the circle formed by the intersection of the surface of the water sphere with the surface of the bounding unit volume. The radiuses r_s , r_w are found from the Pythagorean theorem:

$$r_s = \sqrt{R_s^2 - 0.25}$$

$$r_w = \sqrt{R_w^2 - 0.25}$$
(2)

From the condition that each soil particle has at least an infinitely small area of contact with another particle, the minimum radius of the soil sphere in the model is half the size of a unit cube. The maximum radius should not exceed half the diagonal:

$$\begin{cases} R_{s,\min} = 0.5 \\ R_{s,\max} = \frac{\sqrt{2}}{2} \end{cases}$$
(1)

The volume of mineral particles is calculated as the volume of a sphere of radius R_s truncated by six sectors of height $R_s - 0.5$ (Figure 5, 6).

$$V_s = 1 - n = \frac{4}{3}\pi R_s^3 - 6 \cdot \frac{1}{3}\pi (2R_s^3 - 1.5R_s^2 + 0.125)$$
(2)

Considering porosity equation, the following equation is obtained:

$$n = 8/3\pi R_s^3 - 3\pi R_s^2 + 0.25\pi + 1$$
(3)

A high-order polynomial was obtained in the interval $0.5 \geq R_s \geq \sqrt{2}/2$ to find the inverse function $R_s = f(n)$:

$$R_s = 120.69n^6 - 207.91n^5 + 144.64n^4 - 52.55n^3 + 10.972n^2 - 1.727n + 0.7553$$
(4)

Further, the maximum and minimum soil porosity were obtained, for which this model is applicable:

$$\begin{cases} R_{s,\min} = 0.5 \rightarrow n_{\max} = 0.4764 \\ R_{s,\max} = \frac{\sqrt{2}}{2} \rightarrow n_{\min} = 0.0349 \end{cases}$$
(5)

The proposed model does not allow calculating the thermal conductivity of soil with a porosity of more than 0.4764. It should be noted that soils with a porosity of less than 0.0349 are extremely rare. Since the water is located around the soil particle, the radius of the water sphere must be greater than or equal to the radius of the soil particle. That. The boundaries of the radius of the water sphere for the model:

$$\begin{cases} R_w \geq R_s \\ R_w = 0.5 \rightarrow S_r = 0 \\ R_w = \frac{\sqrt{3}}{2} \rightarrow S_r = 1 \end{cases}$$
(6)

The model is divided into three design cases, to obtain an analytical solution. For each design case, the main design parameters were obtained. Design cases are highlighted due to the geometric features of the model and are determined by a set of conditions:

1. First case:

$$\begin{cases} R_{w,\min} = 0.5 \\ R_{w,\max} = \frac{\sqrt{2}}{2} \end{cases}$$
(7)

2. Second case:

$$\begin{cases} R_w^2 - R_s^2 \geq 0.25 \\ R_{w,\min} = \frac{\sqrt{2}}{2} \\ R_{w,\max} = \frac{\sqrt{3}}{2} \end{cases} \quad (8)$$

3. Third case:

$$\begin{cases} R_w^2 - R_s^2 \leq 0.25 \\ R_{w,\min} = \frac{\sqrt{2}}{2} \\ R_{w,\max} = \frac{\sqrt{3}}{2} \end{cases} \quad (9)$$

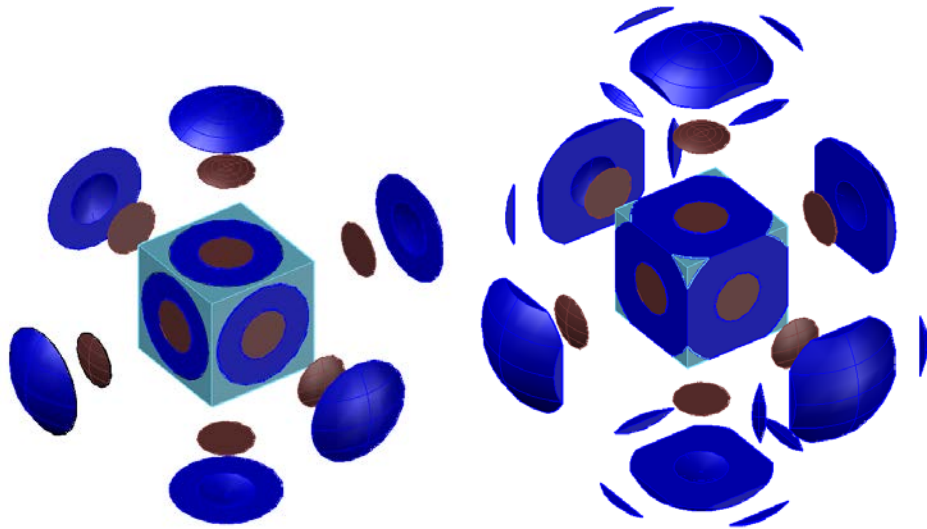


Figure 6. Scheme of truncation of the sphere of water and soil by a unit cube for first design case (left), 2 and 3 cases (right).

For the first computational case, the volume of a sphere with a radius R_w , truncated by the edges of a unit cube, includes the volumes of water and soil particles. For this case, the following expression is valid:

$$V_s + V_w = 1 - n + nS_r = \frac{4}{3}\pi R_w^3 - 6 \cdot \frac{1}{3}\pi (2R_w^3 - 1.5R_w^2 + 0.125) \quad (10)$$

From this equation, the range of admissible values of S_r for the first design case is obtained:

$$\begin{cases} R_{w,\min} = 0.5 \rightarrow (n - nS_r)_{\max} = 0.4764 \rightarrow S_r \geq 1 - \frac{0.4764}{n} \\ R_{w,\max} = \frac{\sqrt{2}}{2} \rightarrow (n - nS_r)_{\min} = 0.0349 \rightarrow S_r \leq 1 - \frac{0.0349}{n} \end{cases} \quad (11)$$

Thus, the range of permissible values of the saturation at a given porosity for the first design case is determined by the following equation:

$$S_r \leq 1 - \frac{0.0349}{n} \quad (12)$$

As $a = n - nS_r$, a polynomial for calculating the R_w parameter for the first design case through porosity and saturation is:

$$R_w = 117.55a^6 - 202.64a^5 + 141.18a^4 - 51.424a^3 + 10.784a^2 - 1.7121a + 0.754 \quad (13)$$

For the second and third calculation cases, the volume of a sphere with a radius of R_w , truncated by the edges of a unit cube, also includes the volumes of water and soil particles. The volume of the truncated sphere is calculated as the difference between a sphere with a radius R_w and six segments of the sphere with the addition of the volumes of 12 figures of the intersection of segments V_c :

$$V_s + V_w = 1 - n + nS_r = \frac{4}{3}\pi R_w^3 - \frac{6}{3}\pi(2R_w^3 - 1.5R_w^2 + 0.125) + 12V_c \quad (14)$$

The volume V_c was found by integration in cylindrical coordinates:

$$12V_c = \frac{48}{3}R_w^3 \arctan \frac{\sqrt{R_w^2 - 0.5}}{R_w} + (1 - 12R_w^2) \arctan \sqrt{4R_w^2 - 2} + \sqrt{4R_w^2 - 2} \quad (15)$$

$$n - nS_r = \frac{8}{3}R_w^3 \left(\pi - 6 \arctan \frac{\sqrt{R_w^2 - 0.5}}{R_w} \right) - 3\pi R_w^2 - \quad (16)$$

$$(1 - 12R_w^2) \arctan \sqrt{4R_w^2 - 2} - \sqrt{4R_w^2 - 2} + 0.25\pi + 1$$

From the equation, the interval of admissible values of S_r for the second and third calculated cases can be expressed:

$$\begin{cases} R_{w,\min} = \frac{\sqrt{2}}{2} \rightarrow (n - nS_r)_{\max} = 0.0349 \rightarrow S_r \geq 1 - \frac{0.0349}{n} \\ R_{w,\max} = \frac{\sqrt{3}}{2} \rightarrow (n - nS_r)_{\min} = 0.0000 \rightarrow S_r \leq 1 - \frac{0}{n} = 1 \end{cases} \rightarrow 1 - \frac{0.0349}{n} \leq S_r \leq 1 \quad (17)$$

Further, a polynomial approximation was obtained to calculate the R_w parameter for the second and third calculation cases. The equation uses porosity and saturation as input. The polynomial is split into two sections (Figure 7). The polynomials for the vertical and inclined portions of the function are obtained separately. The applicability of the model is demonstrated in Figure 7.

If $a = n - nS_r \geq 0.000233$:

$$R_w = 1592939271a^6 - 183771126.0476a^5 + 8347971.33a^4 - 190847.7004a^3 + 2375.7524a^2 - 18.6798a + 0.8315 \quad (18)$$

If $a = n - nS_r \leq 0.000233$:

$$R_w = 298924205636208000000a^6 - 426988215430283000a^5 + 235463863173120a^4 - 63097328697a^3 + 8570419.9417a^2 - 618.7835a + 0.8619 \quad (19)$$

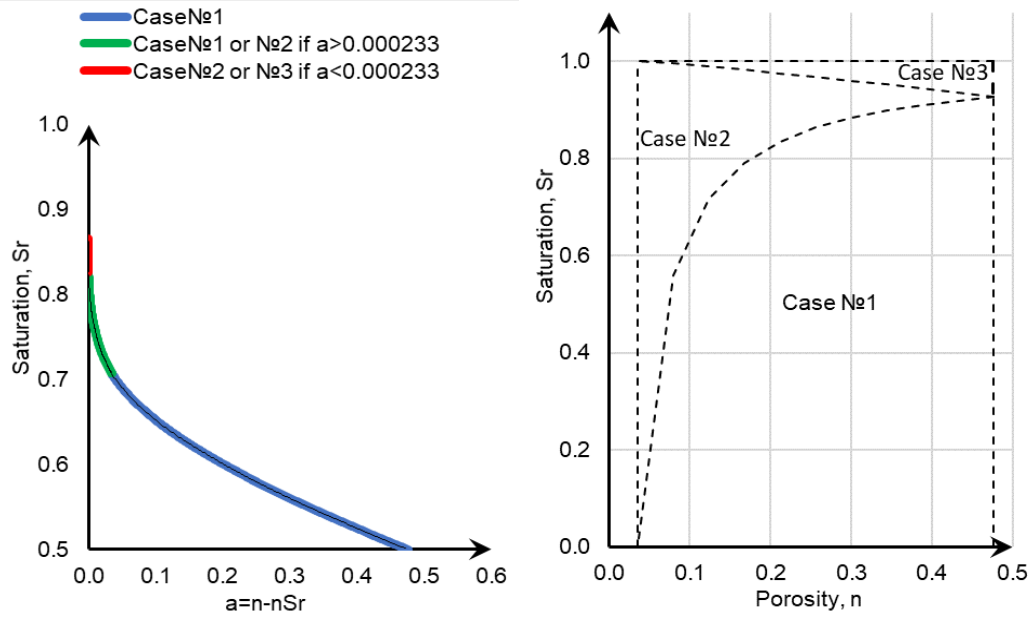
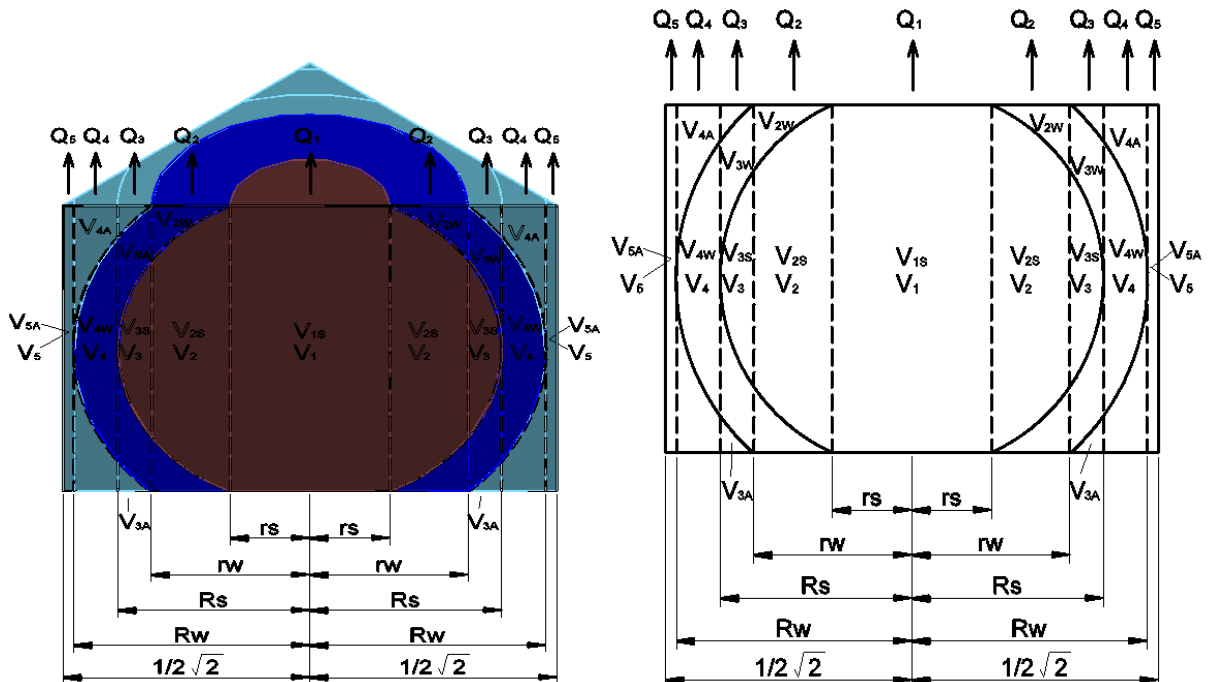


Figure 7. Scope of different cases of model applicability.

A heat flux passing through a unit volume in one direction from bottom to top was considered to derive the heat conduction equation.

The model was divided into volumes in the direction of the heat flow. All volumes have a constant set of components along the path of heat flow. For each case, a separate heat conduction equation is obtained.

For the first design case, five "paths" of the heat flux passing through a unit volume can be distinguished. Design schemes in plan and in section for deriving the desired equation are shown in the Figure 8.



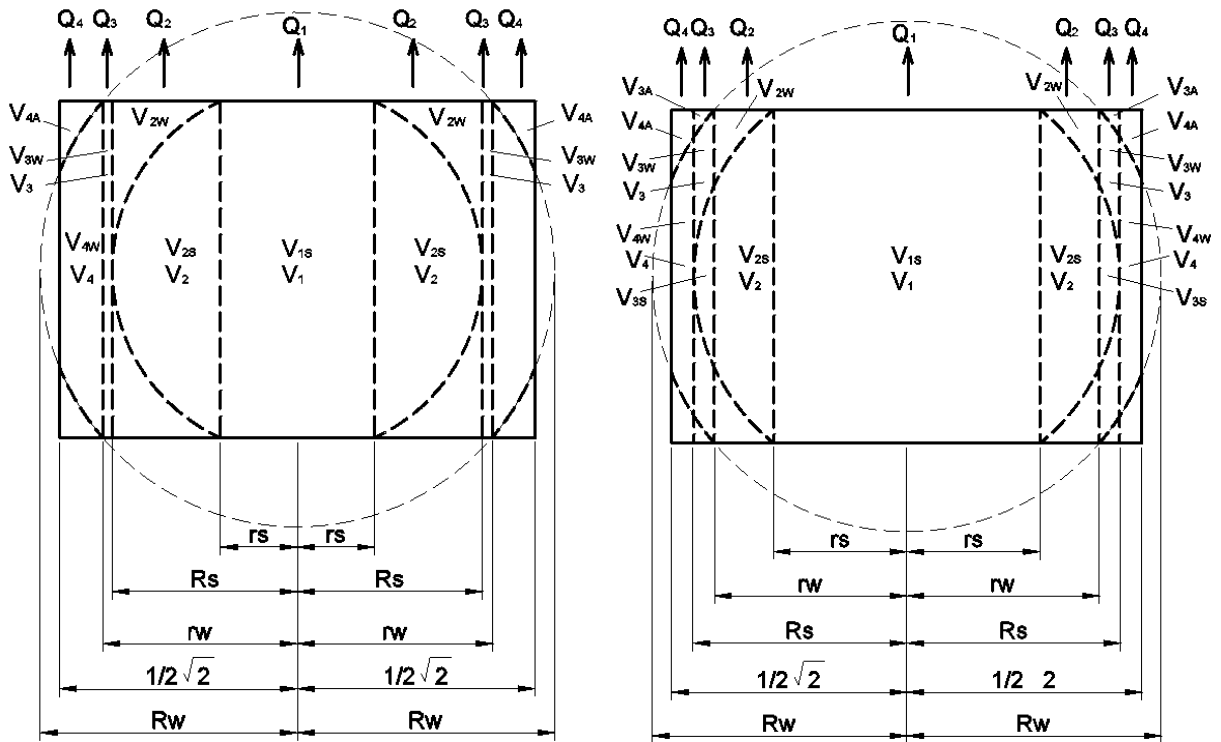


Figure 8. Diagonal section for the first, second, and third design cases.

In Figure 8, the following designations are adopted for the diagrams:

Q_1 is the heat flow passing only through the volume of the mineral part V_{1S} ;

Q_2 is the heat flow passing through the mineral part and water volumes V_{2S} и V_{2W} ;

Q_3 is the heat flow passing through the mineral part, water and air volumes V_{3S} , V_{3W} и V_{3A} ;

Q_4 is the heat flow passing through water and air volumes V_{4W} , V_{4A} ;

Q_5 is the heat flow passing through air volume V_{5A} ;

V_{1-5} is the volume through which heat flows Q_{1-5} pass ;

S_{1-5} is the horizontal sectional areas of volumes V_{1-5}

Thermal conductivity was calculated using the formula:

$$\lambda = \frac{Q}{\Delta T} = \frac{Q_1 + Q_2 + Q_3 + Q_4 + Q_5}{\Delta T} \tag{20}$$

where: ΔT is the temperature gradient, 1 is side length of a unit cube. The values of heat fluxes were found as for a multilayer wall by the formula:

$$Q = S \cdot \frac{\Delta T}{\sum_{i=1}^n \frac{\delta_i}{\lambda_i}} \tag{21}$$

where ΔT is the temperature gradient, S is the heat flow area, δ_i is the thickness of the i -th layer within the area S , λ_i is the thermal conductivity of the i -th layer. Thickness δ_i is considered unchanged within one heat flux:

$$\delta_i = \frac{V_i}{S} \tag{22}$$

With this assumption, the heat flux is written as follows:

$$Q = S^2 \cdot \frac{\Delta T}{\sum_{i=1}^n \frac{V_i}{\lambda_i}} \quad (23)$$

Next, the calculation of the power of heat flows was made for Q_{1-5} :

$$Q_1 = S_1^2 \cdot \frac{\lambda_s \cdot \Delta T}{V_{1S}} \quad (24)$$

$$Q_2 = S_2^2 \cdot \frac{\Delta T}{V_{2S} \div \lambda_s + V_{2W} \div \lambda_w} \quad (25)$$

$$Q_3 = S_3^2 \cdot \frac{\Delta T}{V_{3S} \div \lambda_s + V_{3W} \div \lambda_w + V_{3A} \div \lambda_a} \quad (26)$$

$$Q_4 = S_4^2 \cdot \frac{\Delta T}{V_{4W} \div \lambda_w + V_{4A} \div \lambda_a} \quad (27)$$

$$Q_5 = S_5^2 \cdot \frac{\Delta T}{V_{1S} \div \lambda_s} \quad (28)$$

Combining equations and (25), an expression was obtained to determine the thermal conductivity of the entire model:

$$\lambda = \frac{S_1 \lambda_s}{1} + \frac{S_2^2}{\frac{V_{2S}}{\lambda_s} + \frac{V_{2W}}{\lambda_w}} + \frac{S_3^2}{\frac{V_{3S}}{\lambda_s} + \frac{V_{3W}}{\lambda_w} + \frac{V_{3A}}{\lambda_a}} + \frac{S_4^2}{\frac{V_{4W}}{\lambda_w} + \frac{V_{4A}}{\lambda_a}} + \frac{S_5 \lambda_a}{1} \quad (29)$$

Equations of heat conductivity for second and third calculation cases were obtained in a similar way. For the second and third design cases, four "paths" of the heat flux passing through a unit volume can be distinguished.

$$\lambda = \frac{S_1 \lambda_s}{1} + \frac{S_2^2}{\frac{V_{2S}}{\lambda_s} + \frac{V_{2W}}{\lambda_w}} + \frac{S_3 \lambda_w}{1} + \frac{S_4^2}{\frac{V_{4W}}{\lambda_w} + \frac{V_{4A}}{\lambda_a}} \quad (30)$$

$$\lambda = \frac{S_1 \lambda_s}{1} + \frac{S_2^2}{\frac{V_{2S}}{\lambda_s} + \frac{V_{2W}}{\lambda_w}} + \frac{S_3^2}{\frac{V_{3S}}{\lambda_s} + \frac{V_{3W}}{\lambda_w} + \frac{V_{3A}}{\lambda_a}} + \frac{S_4^2}{\frac{V_{4W}}{\lambda_w} + \frac{V_{4A}}{\lambda_a}} \quad (31)$$

Equations were derived for the geometric parameters of the model S_i and V_i . The calculation was made by the intersection of the coordinate system and the areas of the data element (spheres, cylinder, cube). The individual parameters are calculated by integration in cylindrical coordinates.

3. Results and Discussion

The calculation of thermal conductivity according to the developed model is performed in the following sequence:

1) Preparation of input data. Initial data include saturation, porosity, the thermal conductivity of water, air, and mineral parts. Saturation and porosity can be obtained from laboratory tests. It is permissible to assign thermal conductivity of water and air $\lambda_w = 0.56 \text{ W/m}^\circ\text{C}$, $\lambda_a = 0.026 \text{ W/m}^\circ\text{C}$.

The thermal conductivity of the mineral part λ_s can be determined by carrying out one experimental measurement. When experimentally determining the thermal conductivity of a conventional mineral part, a test is required on a soil sample with a porosity of $n \leq 0.4764$.

The sample can be obtained from field test or formed in the laboratory. It is also crucial that the sample's granulometric and mineralogical composition corresponds to the soil composition for which the calculation will be made. After the experiment, the value of λ_s is selected so that the values of the experimental determination and the calculated one coincide. The found value λ_s will be suitable for calculating thermal conductivity at various values of n and S_r , provided that the mineralogical and particle size distribution is preserved.

When it is not possible to make a test, it is possible to approximately assign the thermal conductivity of the mineral part, based on the quartz content in the soil, using the calculation formulas proposed by Campbell or Johansen.

2) Checking model applicability. Porosity should be less than $n \leq 0.4764$.

3) The choice of the design case of the model according to the value of the saturation:

$$\begin{cases} S_r \leq 1 - \frac{0.0349}{n} \rightarrow \text{case1} \\ S_r \geq 1 - \frac{0.0349}{n} \rightarrow \text{case2or3} \end{cases} \quad (32)$$

4) Determination of the design parameters R_s and R_w according to the formulas of the corresponding design case. At this stage, a choice is made between the second and third design cases:

$$\begin{cases} R_w^2 - R_s^2 \geq 0.25 \rightarrow \text{case2} \\ R_w^2 - R_s^2 \leq 0.25 \rightarrow \text{case3} \end{cases} \quad (33)$$

5) Calculation of the model's parameters S_i and V_i according to the formulas of Tables 1-3 for the corresponding design case.

Table 1. Equations of thermal conductivity parameters for first a design case.

| Parameters | Calculation formula |
|------------|--|
| S_1 | $\pi(R_s^2 - 0.25)$ |
| S_2 | $\pi(R_w^2 - R_s^2)$ |
| S_3 | $\pi(R_s^2 - R_w^2 + 0.25) - 4R_s^2 \arccos\left(\frac{0.5}{R_s}\right) + 2\sqrt{R_s^2 - 0.25}$ |
| S_4 | $1 - S_1 - S_2 - S_3 - S_5$ |
| S_5 | $1 - \pi R_w^2 + 4R_w^2 \arccos\left(\frac{0.5}{R_w}\right) - 2\sqrt{R_w^2 - 0.25}$ |
| V_{2S} | $\frac{4}{3}\pi \left[0.125 - (R_s^2 - R_w^2 + 0.25)^{\frac{3}{2}} \right]$ |
| V_{3S} | $\frac{4}{3}\pi \left[(R_s^2 - R_w^2 + 0.25)^{\frac{3}{2}} - 2R_s^3 + 1.5R_s^2 - 0.125 \right]$ |

| Parameters | Calculation formula |
|------------|--|
| V_{2W} | $\pi(R_w^2 - R_s^2) - \frac{4}{3}\pi \left[0.125 - (R_s^2 - R_w^2 + 0.25)^{\frac{3}{2}} \right]$ |
| V_{3W} | $n \cdot S_r - V_{2W} - V_{4W}$ |
| V_{4W} | $-\frac{8}{3}\pi R_w^3 + 2\pi R_w^2 - \frac{1}{6}\pi + \frac{16}{3}(R_w^2 - R_s^2)^{\frac{3}{2}} \cdot \left(\frac{\pi}{4} - \arccos \frac{1}{2R_s} \right) +$ $\frac{16}{3}R_w^3 \arctan \left(2R_w \sqrt{\frac{R_s^2 - 0.25}{R_w^2 - R_s^2}} \right) -$ $\frac{4}{3}(3R_w^2 - 0.25) \arcsin \sqrt{\frac{R_s^2 - 0.25}{R_w^2 - 0.25}} - \frac{4}{3} \sqrt{R_s^2 - 0.25} \sqrt{R_w^2 - R_s^2}$ |
| V_{3A} | $S_3 \cdot 1$ |
| V_{4A} | $S_4 \cdot 1$ |

Table 2. Equations of thermal conductivity parameters for a second design case.

| Parameters | Calculation formula |
|------------|--|
| S_1 | $\pi(R_s^2 - 0.25)$ |
| S_2 | $0.25\pi - 4R_s^2 \arccos \left(\frac{0.5}{R_s} \right) + 2\sqrt{R_s^2 - 0.25}$ |
| S_3 | $1 - S_1 - S_2 - S_4$ |
| S_4 | $\frac{1}{4}\pi + 1 - \pi R_w^2 + 4(R_w^2 - 0.25) \arccos \left(\frac{0.5}{\sqrt{R_w^2 - 0.25}} \right) - 2\sqrt{R_w^2 - 0.5}$ |
| V_{2S} | $S_2 \cdot 1 - V_{2W}$ |
| V_{3S} | - |
| V_{2W} | $nS_r - V_{3W} - V_{4W}$ |
| V_{3W} | $\pi(R_w^2 - R_s^2 - 0.25) - 4(R_w^2 - 0.25) \arccos \left(\frac{0.5}{\sqrt{R_w^2 - 0.25}} \right) + 4R_s^2 \arccos \left(\frac{0.5}{R_s} \right) +$ $2\sqrt{R_w^2 - 0.5} - 2\sqrt{R_s^2 - 0.25}$ |
| V_{4W} | $S_4 \cdot 1 - V_{4A}$ |
| V_{4A} | $n - nS_r$ |

Table 3. Equations of thermal conductivity parameters for a third design case.

| Parameters | Calculation formula |
|------------|--|
| S_1 | $\pi(R_s^2 - 0.25)$ |
| S_2 | $\pi(R_w^2 - R_s^2) - 4(R_w^2 - 0.25) \arccos\left(\frac{0.5}{\sqrt{R_w^2 - 0.25}}\right) + 2\sqrt{R_w^2 - 0.5}$ |
| S_3 | $1 - S_1 - S_2 - S_4$ |
| S_4 | $1 - \pi R_s^2 + 4R_s^2 \arccos\left(\frac{0.5}{R_s}\right) - 2\sqrt{R_s^2 - 0.25}$ |
| V_{2S} | $1 - n - V_{1S} - V_{3S}$ |
| V_{3S} | $-\frac{8}{3}\pi R_s^3 + 2\pi R_s^2 - \frac{1}{6}\pi + \frac{16}{3}(R_s^2 - R_w^2 + 0.25)^{\frac{3}{2}} \cdot \left(\frac{\pi}{4} - \arccos\frac{1}{2\sqrt{R_w^2 - 0.25}}\right) +$ $\frac{16}{3}R_s^3 \arctan\left(2R_s\sqrt{\frac{R_w^2 - 0.5}{R_s^2 - R_w^2 + 0.25}}\right) - \frac{4}{3}(3R_s^2 - 0.25) \arcsin\sqrt{\frac{R_w^2 - 0.5}{R_s^2 - 0.25}} -$ $\frac{4}{3}\sqrt{R_w^2 - 0.5}\sqrt{R_s^2 - R_w^2 + 0.25}$ |
| V_{2W} | $S_2 \cdot 1 - V_{2S}$ |
| V_{3W} | $nS_r - V_{2W} - V_{4W}$ |
| V_{4W} | $\frac{16}{3}R_w^3 \left(\arctan\left(\frac{R_w\sqrt{4R_s^2 - 1}}{\sqrt{R_w^2 - R_s^2}}\right) - \arctan\left(\frac{R_w}{\sqrt{R_w^2 - 0.5}}\right) \right) +$ $\frac{1}{3}(12R_w^2 - 1) \left(\arcsin\left(\frac{1}{\sqrt{4R_w^2 - 1}}\right) - \arcsin\left(\sqrt{\frac{R_s^2 - 0.25}{R_w^2 - 0.25}}\right) \right) +$ $\frac{2}{3}\left(\sqrt{R_w^2 - 0.5} - 2\sqrt{R_s^2 - 0.25}\sqrt{R_w^2 - R_s^2}\right) + \frac{16}{3}(R_w^2 - R_s^2)^{\frac{3}{2}} \left(\frac{\pi}{4} - \arccos\frac{0.5}{R_s}\right)$ |
| V_{3A} | $n - nS_r - V_{4A}$ |
| V_{4A} | $S_4 \cdot 1 - V_{4W}$ |

According to the proposed model, the thermal conductivity for sand and clay was calculated at various parameters of porosity and saturation. Thermal conductivity of water and air are $\lambda_w = 0.56$ W/m°C and $\lambda_a = 0.026$ W/m°C. Thermal conductivity of the mineral part $\lambda_s = 3.85$ W/m°C for clay and $\lambda_s = 8.1$ W/m°C for sand. Variation of the saturation is 0–1. The porosity varied within 0.05–0.45.

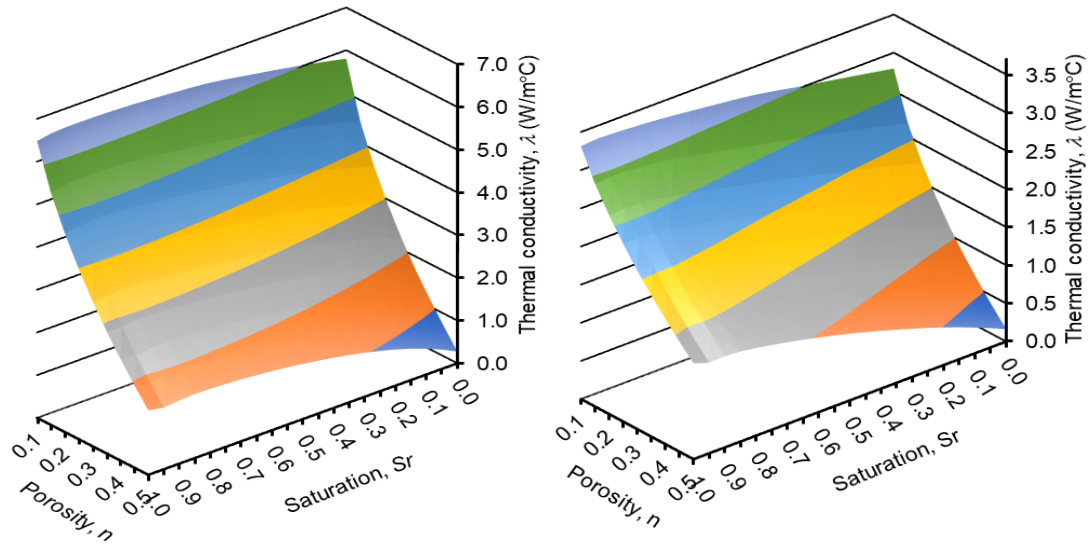
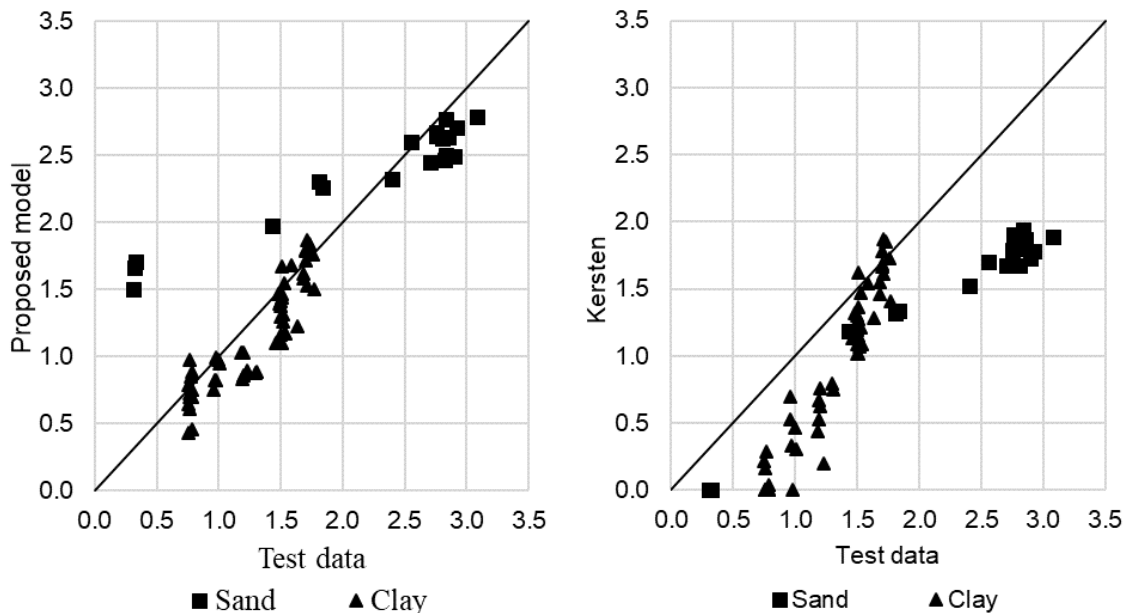


Figure 9. Thermal conductivity for sand (left) and clay (right) calculated at various parameters of porosity and saturation.

The reliability was assessed by comparing the results of the calculation of thermal conductivities according to the proposed model with experimental data and comparing the results of the calculation according to several generally accepted models.

For these purposes, an array of data on thermal conductivity of cohesive and sandy soils with varying porosity and saturation was formed. The dataset was obtained by laboratory measurements of thermal conductivity for sandy and clayey soils.

To assess the effectiveness of the proposed model, the calculation results were compared with other most popular models for assessing the thermal conductivity of the soil. For comparison, the models proposed by Kersten [18], Mickley [7], De Vries [8], Gemant [2], McGaw [9], Campbell [11], Johansen [19] were used. The comparison results are shown in Figure 10.



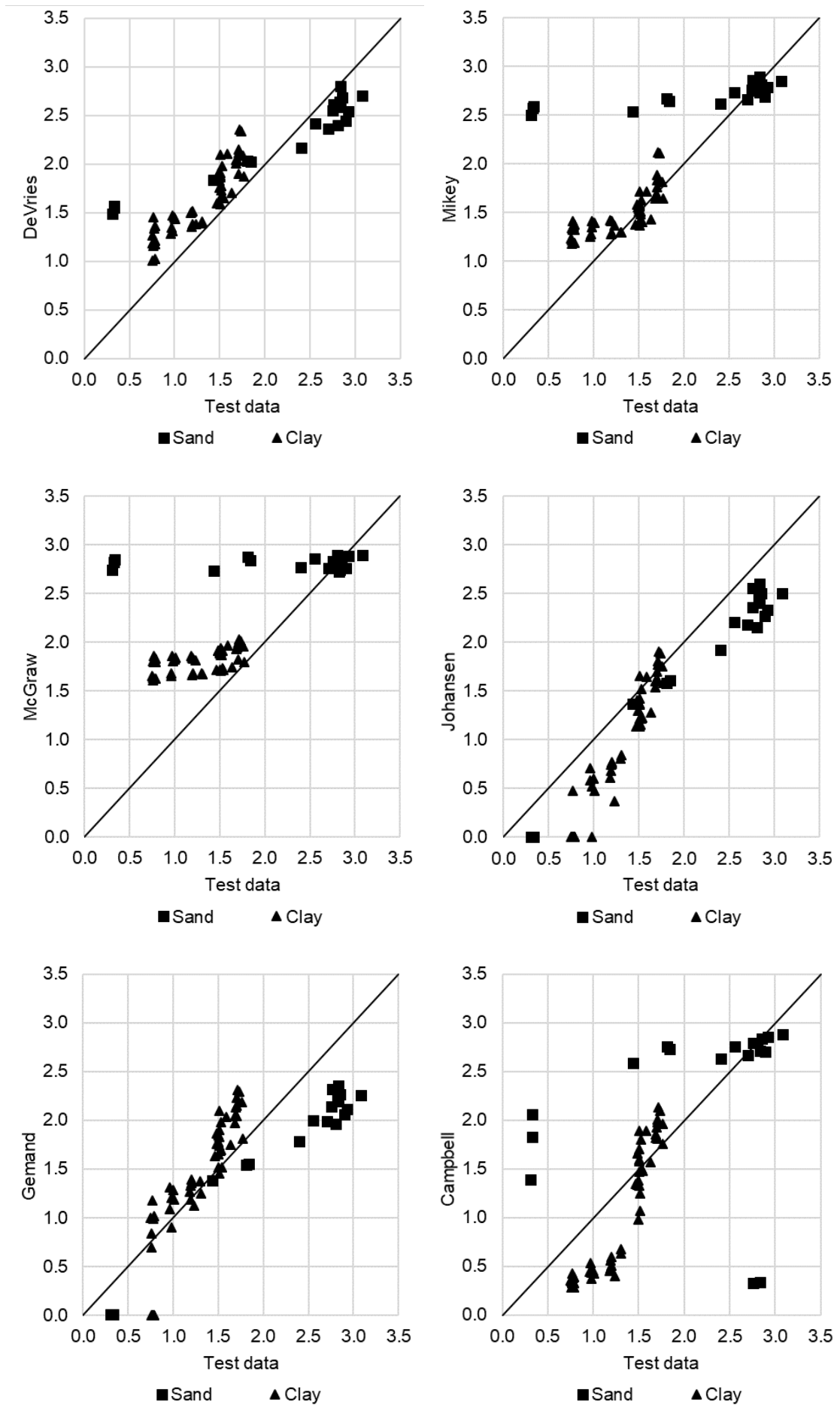


Figure 10. The comparison results.

To evaluate the performance of the proposed model, a number of statistical indicators were calculated. Pearson correlation coefficient, mean absolute percentage error and mean squared error are presented in the Table 4.

Table 4. Comparison of calculated data with experimental.

| Calculation method | Sand | | | Clay | | |
|--------------------|------|----------|--------|------|----------|-------|
| | MSE | Pirson R | MAPE | MSE | Pirson R | MAPE |
| Kersten | 0.89 | 0.95 | 32.19 | 0.19 | 0.93 | 22.48 |
| De Vries | 0.30 | 0.96 | 67.24 | 0.14 | 0.90 | 47.43 |
| Mickley | 0.93 | 0.81 | 119.00 | 0.09 | 0.76 | 24.51 |
| McGraw | 1.18 | 0.15 | 133.20 | 0.38 | 0.55 | 53.22 |
| Johansen | 0.19 | 0.94 | 15.19 | 0.11 | 0.92 | 21.77 |
| Gemand | 0.39 | 0.93 | 21.66 | 0.09 | 0.92 | 18.48 |
| Lu et al. 2014 | 0.82 | 0.98 | 42.31 | 0.43 | 0.83 | 45.39 |
| Campbell | 0.02 | 0.99 | 19.95 | 0.17 | 0.93 | 30.70 |
| Proposed model | 0.34 | 0.97 | 21.78 | 0.05 | 0.90 | 18.05 |

To evaluate the performance of the proposed model, a number of statistical indicators were calculated. Pearson correlation coefficient, mean absolute percentage error and mean squared error are presented in the table.

Analysis of the above graphs and tables shows that for sandy soils, the Proposed model, the models of Johansen, Gemand and Campbell have good agreement with the experimental data and a low error.

For clayey soils, the Proposed model, the models of Johansen, Gemand and Kersten have good agreement with the experimental data and a low error.

4. Conclusion

Based on the results of the development of the model, the following conclusions were made:

1) The developed computational model for determining the thermal conductivity of the soil makes it possible to take into account the three-phase structure of the soil and the variable contact area of the mineral parts.

2) An analytical solution has been obtained, and a calculation method has been proposed, making it possible to assess the thermal conductivity of the soil based on its physical characteristics - porosity and saturation.

3) The proposed technique makes it possible to increase the convergence of the results with experimental data by determining the parameter from single laboratory determinations of the thermal conductivity of the soil.

References

1. Ponomaryov, A.B., Zakharov, A.V. Numerical Simulation of the Process of the Geothermal Low-potential Ground Energy Extraction in the Perm Region (Russia). *Procedia Engineering*. 2016. DOI: 10.1016/j.proeng.2016.07.293
2. Gemant, A. How to compute thermal soil conductivities. *Heating, Piping and Air Conditioning*. 1952. 24(1). Pp. 122–123.
3. Tarnawski, V.R., Momose, T., Leong, W.H. Assessing the impact of quartz content on the prediction of soil thermal conductivity. *Geotechnique*. 2009. 59(4). Pp. 331–338. DOI: 10.1680/geot.2009.59.4.331
4. Aduda, B.O. Effective thermal conductivity of loose particulate systems. *Journal of Materials Science*. 1996. 31(24). Pp. 6441–6448. DOI: 10.1007/BF00356246
5. Esch, D.C. Thermal analysis, construction, and monitoring methods for frozen ground 2013. 1–492 p. ISBN:9780784475485.
6. Dong, Y., McCartney, J.S., Lu, N. Critical Review of Thermal Conductivity Models for Unsaturated Soils. *Geotechnical and Geological Engineering*. 2015. 33(2). Pp. 207–221. DOI: 10.1007/s10706-015-9843-2
7. Mickley, A.S. The Thermal Conductivity of Moist Soil. *Transactions of the American Institute of Electrical Engineers*. 1951. 70(2). Pp. 1789–1797. DOI: 10.1109/T-AIEE.1951.5060631
8. De Vries D.A. The thermal conductivity of soil. *Mededeelingen van de Landbouwhogeschool te Wageningen*. Translated by Building Research Station (Library Communication No. 759). 1952. 52(1). Pp. 1–73.

9. MCGAW R. Heat Conduction in Saturated Granular Materials. Nat Acad Sciences-Nat Research Council--Highway Research Board--Special Report 103. 1969. Pp. 114–131.
10. Gori, F., Corasaniti, S. Theoretical prediction of the soil thermal conductivity at moderately high temperatures. *Journal of Heat Transfer*. 2002. 124(6). Pp. 1001–1008. DOI: 10.1115/1.1513573
11. Campbell, G.S., Jungbauer, J.D., Bidlake, W.R., Hungerford, R.D. Predicting the effect of temperature on soil thermal conductivity. *Soil Science*. 1994. 158(5). Pp. 307–313. DOI: 10.1097/00010694-199411000-00001
12. Gens, A., Sánchez, M., Guimarães, L.D.N., Alonso, E.E., Lloret, A., Olivella, S., Villar, M. V., Huertas, F. A full-scale in situ heating test for high-level nuclear waste disposal: Observations, analysis and interpretation. *Geotechnique*. 2009. 59(4). Pp. 377–399. DOI: 10.1680/geot.2009.59.4.377
13. Cho, W.J., Lee, J.O., Kwon, S. An empirical model for the thermal conductivity of compacted bentonite and a bentonite-sand mixture. *Heat and Mass Transfer/Waerme- und Stoffuebertragung*. 2011. 47(11). Pp. 1385–1393. DOI: 10.1007/s00231-011-0800-1.
14. Haigh, S.K. Thermal conductivity of sands. *Geotechnique*. 2012. 62(7). Pp. 617–625. DOI: 10.1680/geot.11.P.043
15. Tarnawski, V.R., Leong, W.H. Advanced Geometric Mean Model for Predicting Thermal Conductivity of Unsaturated Soils. *International Journal of Thermophysics*. 2016. 37(2). Pp. 1–42. DOI: 10.1007/s10765-015-2024-y
16. Tian, Z., Lu, Y., Horton, R., Ren, T. A simplified de Vries-based model to estimate thermal conductivity of unfrozen and frozen soil. *European Journal of Soil Science*. 2016. 67(5). Pp. 564–572. DOI: 10.1111/ejss.12366
17. Lu, Y., Lu, S., Horton, R., Ren, T. An Empirical Model for Estimating Soil Thermal Conductivity from Texture, Water Content, and Bulk Density. *Soil Science Society of America Journal*. 2014. 78(6). Pp. 1859–1868. DOI: 10.2136/sssaj2014.05.0218
18. Kersten, M.S. Thermal properties of soils. 30th Annual Meeting of the Highway Research Board. 1952. Pp. 161–166.
19. Johansen, O. Thermal Conductivity of Soils and Rocks. Sixth International Congress of the Foundation Francaise d'Etudes Nordiques. 1975. 2. Pp. 407–420.
20. Knutsson, S. On the Thermal Conductivity and Thermal Diffusivity of Highly Compacted Bentonite. (October)1983. 72–83 p.
21. Côté, J., Konrad, J.M. A generalized thermal conductivity model for soils and construction materials. *Canadian Geotechnical Journal*. 2005. 42(2). Pp. 443–458. DOI: 10.1139/t04-106
22. Nikoosokhan, S., Nowamooz, H., Chazallon, C. Effect of dry density, soil texture and time-spatial variable water content on the soil thermal conductivity. *Geomechanics and Geoengineering*. 2016. 11(2). Pp. 149–158. DOI: 10.1080/17486025.2015.1048313
23. Zhang, N., Wang, Z. Review of soil thermal conductivity and predictive models. *International Journal of Thermal Sciences*. 2017. 117. Pp. 172–183. DOI: 10.1016/j.ijthermalsci.2017.03.013
24. Dharssi, I., Vidale, P.L., Verhoef, A., Macpherson, B., Jones, C., Best, M. New soil physical properties implemented in the Unified Model at PS18. (528)2009. 35 pp.
25. Wilson, J., Savage, D., Bond, A., Watson, S., Bennet, D. Bentonite: A review of key properties, processes and issues for consideration in the UK context. 1(February)2011. 1–6 p.
26. Rózański, A., Stefaniuk, D. On the prediction of the thermal conductivity of saturated clayey soils: Effect of the specific surface area. *Acta Geodynamica et Geomaterialia*. 2016. 13(4). Pp. 339–349. DOI: 10.13168/AGG.2016.0016
27. Rózański, A., Kaczmarek, N. Empirical and theoretical models for prediction of soil thermal conductivity: A review and critical assessment. *Studia Geotechnica et Mechanica*. 2020. 42(4). Pp. 330–340. DOI: 10.2478/sgem-2019-0053
28. McCumber, M.C., Pielke, R.A. Simulation of the effects of surface fluxes of heat and moisture on a mesoscale numerical model. 1. Soil layer. *Journal of Geophysical Research*. 1981. 86(C10). Pp. 9929–9938. DOI: 10.1029/JC086iC10p09929
29. Kahr G., M.-V.M. Thermal conductivity of Bentonite MX 80 and Montigel using the heating wire method.
30. Chung, S. -O, Horton, R. Soil heat and water flow with a partial surface mulch. *Water Resources Research*. 1987. 23(12). Pp. 2175–2186. DOI: 10.1029/WR023i012p02175
31. Misra, A., Becker, B.R., Fricke, B.A. A Theoretical model of the thermal conductivity of idealized soil. *HVAC and R Research*. 1995. 1(1). Pp. 81–96. DOI: 10.1080/10789669.1995.10391310
32. Newson, T.A., Brunning, P., Stewart, G. Thermal conductivity of consolidating offshore clayey backfill. *Proceedings of the International Conference on Offshore Mechanics and Arctic Engineering - OMAE*. 2002. 4. Pp. 17–24. DOI: 10.1115/OMAE2002-28020
33. Caridad, V., Ortiz de Zárate, J.M., Khayet, M., Legido, J.L. Thermal conductivity and density of clay pastes at various water contents for pelotherapy use. *Applied Clay Science*. 2014. 93–94. Pp. 23–27. DOI: 10.1016/j.clay.2014.02.013
34. Yoon, S., Cho, W.H., Lee, C., Kim, G.Y. Thermal conductivity of Korean compacted bentonite buffer materials for a nuclear waste repository. *Energies*. 2018. 11(9). DOI: 10.3390/en11092269
35. Nimick, F.B., Leith, J.R. A model for thermal conductivity of granular porous media. *Journal of Heat Transfer*. 1992. 114(2). Pp. 505–508. DOI: 10.1115/1.2911302
36. Jougnot, D., Revil, A. Thermal conductivity of unsaturated clay-rocks. *Hydrology and Earth System Sciences*. 2010. 14(1). Pp. 91–98. DOI: 10.5194/hess-14-91-2010
37. Yun, T.S. Mechanical and thermal study of hydrate bearing sediments. (August)2005.
38. Ewing, R.P., Horton, R. Thermal conductivity of a cubic lattice of spheres with capillary bridges. *Journal of Physics D: Applied Physics*. 2007. 40(16). Pp. 4959–4965. DOI: 10.1088/0022-3727/40/16/031
39. Gori, F., Corasaniti, S. New model to evaluate the effective thermal conductivity of three-phase soils. *International Communications in Heat and Mass Transfer*. 2013. 47. Pp. 1–6. DOI: 10.1016/j.icheatmasstransfer.2013.07.004
40. Ofrikhter, I., Zaharov, A., Ponomaryov, A., Likhacheva, N. Modeling heat transfer process in soils. *MATEC Web of Conferences*. 2018. DOI: 10.1051/mateconf/201825102048

Information about authors:

Aleksandr Zakharov

PhD in Technical Science

ORCID: <https://orcid.org/0000-0001-7475-8779>

E-mail: av_zaharov@mail.ru

Andrey Ponomaryov

Doctor in Technical Science

ORCID: <https://orcid.org/0000-0001-6521-9423>

E-mail: andreypab@mail.ru

Ian Ofrikhter

ORCID: <https://orcid.org/0000-0002-3703-5878>

E-mail: ian.ofrikhter@gmail.com

Received 22.10.2021. Approved after reviewing 31.05.2022. Accepted 07.06.2022.